

Performance Evaluation Experiments on a Laser Spot Triangulation Probe

Bala Muralikrishnan, Wei Ren, Dennis Everett, Eric Stanfield and Ted Doiron
Semiconductor and Dimensional Metrology Division
National Institute of Standards and Technology, Gaithersburg MD 20899

Contact information: balam@nist.gov, 301-975-3789 (phone), 301-869-0822 (fax)

Abstract

Laser triangulation probes are increasingly used for dimensional measurements in a variety of applications. At the National Institute of Standards and Technology, we have recently explored the use of laser spot triangulation probes to determine dimensional features such as height and width of channels in a fuel cell plate. To assess the suitability of the probes for performing these dimensional measurements, we designed several experiments that highlighted different error sources in the probes. This report is a summary of those experiments. Numerous studies have been reported in the literature on error sources in laser triangulation probes utilizing artifacts of varying shape (form), color, reflectivity, surface finish, etc. However, our experiments are targeted towards establishing bounds on errors when measuring simple linear dimensions such as height and width on prismatic objects of a single color and material. Our scope is indeed narrow, but intentionally so; it is our objective to highlight the influence of a number of “hidden performance attributes” [1] that impact accuracy of even simple linear dimensional measurements so that it may be of use to others who perform similar measurements.

1. Introduction

Laser triangulation probes are increasingly considered as a viable alternative to touch probes for rapid dimensional measurements in a variety of applications. While they are indeed inexpensive to procure and operate, the achievable accuracy in the measurements is influenced by numerous “hidden performance attributes” as pointed out by Buzinski et al [1], which are often not clearly specified by the manufacturer of the probes.

Recently, we explored the use of laser triangulation probes for measuring channel height and width of bipolar fuel cell plates. In order to evaluate the suitability of these probes for our application, we attempted to estimate the influence of different sources of error through carefully designed experiments. In effect, our experiments highlighted the different “hidden performance attributes” such as the “accuracy with which edges can be located”, “ability to reject erroneous measurements caused by image distortion” [1], and other attributes not discussed in [1] such as the effect of spot size and shape, material penetration of the laser, linearity error, etc. While Buzinski et al [1] present qualitative results, we have attempted to provide bounds for errors, at least to the extent that it pertains to our application involving simple linear dimensional measurements. We summarize the results of these experiments in this report with the hope that such targeted testing will be of value to other users of laser triangulation probes.

Laser triangulation probes do suffer from numerous error sources; Garces et al [2] present an excellent review of those errors. There is also literature [1-9] that describes experiments to evaluate the performance of triangulation probes; several experiments described therein are sensitive to different error sources in the probe. The primary difference between the prior work reported in the literature and our report here is that while most prior studies have a broad focus encompassing such effects as material/optical properties, surface finish, reflectivity, color, ambient light, part shape and form, etc, on measurement errors, our study is of a much narrower focus. We have only attempted to consider those factors that may potentially influence height and width measurements on objects of homogenous material where surface finish, reflectivity, color, etc do not change from one position to another and therefore produce common-mode errors which can theoretically be calibrated out. Even in this restricted sense, our experiments do show that the influence quantities that we have considered can have a profound effect on dimensional measurements.

Our experiments were performed with a spot probe and therefore we integrated a linear translation stage (Aerotech ALS 50060 [10]) that can scan the object against the stationary probe to obtain a profile. The linear stage has a high positioning accuracy encoder (accuracy specification of $\pm 1 \mu\text{m}$), which was verified using a laser interferometer. In order to synchronize the data from the laser triangulation probe and the encoder, we utilized the Position Synchronized Output (PSO) facility of the stage. The pulses from the PSO were used to trigger data acquisition from the analog output port of the probe's controller. Even though the encoder has a resolution of 20 nm, we only attempt to acquire a data point at approximately every $1 \mu\text{m}$ interval. For information purposes, we also mention that the stage has a straightness specification of $\pm 3 \mu\text{m}$, and a pitch and yaw specification of 17 arc-seconds.

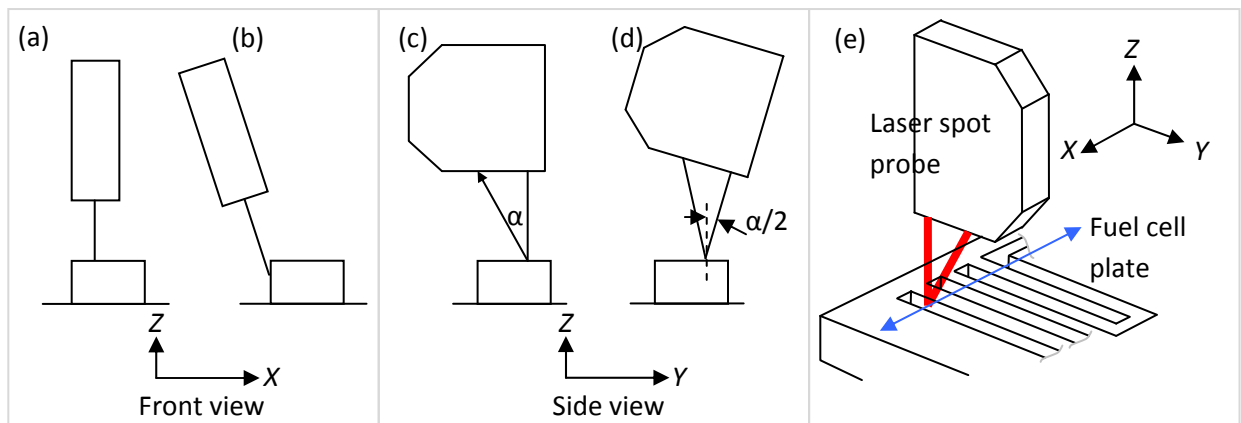


Fig. 1 Part is scanned along the X axis. Front view shown in (a) and (b). Side view shown in (c) and (d). (a) The probe is oriented so that its laser is incident normal to the surface (b) The probe is tilted in the XZ plane so that the probe can acquire data from the side wall as the part is scanned along X (c) Probe has no tilt in the YZ plane. This situation corresponds to measurement of diffuse surfaces. (d) Probe is tilted in the YZ plane to measure specular surfaces. (e) 3D view of the probe measuring height and width of a fuel cell plate. Notice that the plane of the probe's measurement triangle (YZ plane) is orthogonal to the axis of travel (along X).

Before we proceed with an outline of our experiments, we note two aspects worthy of attention. First, while some of our experiments highlight error sources that are probably common to most laser triangulation probes, others revealed peculiarities that were specific to the Keyence [10] LK-G32 probe and its associated controller, the LK-GD500. Second, the probe can be mounted in different orientations with respect to the object under test. The angular orientation of the probe can have a significant bearing on the accuracy of the results. Possible configurations of the probe and part are shown in Fig. 1. For all experiments we have considered, the plane of the probe's measurement triangle (the YZ plane in Fig. 1(e)) is normal to the axis of travel (the X axis). It is only in this arrangement that this plane is not obstructed by the part as it enters a depth feature.

2. Outline

This report is organized as follows. Section 3 describes experiments that identify error sources that are likely common to different triangulation probes, although we may have invoked performance specifications for the Keyence LK-G32 probe in some instances. Section 4 describes some issues that are specific to the Keyence LK-G32 probe and its controller, the LK-GD500. An outline of the experiments is given below:

Section 3: Experiments that highlight common error sources in most triangulation probes

- 3.1 Repeatability and noise levels
- 3.2 Linearity experiments
- 3.3 Influence of material/optical properties on height measurements
- 3.4 Influence of material/optical properties on width measurements
- 3.5 Effect of spot size on width measurements
- 3.6 Side wall reflections
- 3.7 Secondary reflections
- 3.8 Measurements at grazing angle

Section 4: Issues specific to our Keyence LK-G32 probe and LK-GD500 controller

- 4.1 Analog output from the controller
- 4.2 Delay
- 4.3 Software issues such as alarm, averaging, etc
- 4.3 Controller noise

3. Experiments that highlight common error sources in most triangulation probes

We describe experiments that highlight common error sources in most triangulation probes in this section.

3.1 Repeatability and noise levels

The single point repeatability of the probe for data acquired over several seconds (at a sampling rate of 50 μ s) is slightly less than 1 μ m (one standard deviation) for the probe that we tested. The manufacturer's specification of 50 nm is valid when a moving average filter of 256 data points is applied. The data from the analog output port has a noise level in the ± 2 μ m range. We should point out that height measurements are performed by averaging numerous data points on the two

defining edges of the height feature, and therefore the repeatability will not be a significant contributor to the overall error. Width measurements, on the other hand, may be performed in two different ways. If the probe is positioned as in Fig. 1(a), the edge is determined by a single data point and the probe's ranging repeatability is of no consequence, but the finite spot size will limit the lateral resolution achievable as we show in section 3.5. If however, the probe is positioned as shown in Fig. 1(b) and data points are acquired along the side wall also, then the probe's ranging repeatability does impact width measurements, but only the component along the X axis will influence the result. Again, averaging will reduce the influence of this term.

Implications for dimensional measurements: The repeatability of the probe is not anticipated to be a major source of error in height and width measurements because of the significant averaging that occurs in their calculation.

3.2 Linearity experiments

The linearity error (E) of the probe is specified to be $\pm 5 \mu\text{m}$ over the full travel of 10 mm for the Keyence LK-G32. The scale error in the probe is calibrated using gage blocks of known height and therefore removed. The scale error is defined as the linear term in the error during measurement while the linearity error is the residual from the best-fit line to the scale error.

This specification of $\pm 5 \mu\text{m}$ is based on normal incidence on a white ceramic target. Most applications will involve situations where neither the normal incidence nor the white ceramic criteria is met. We therefore performed some tests to determine the linearity error of the probe for a variety of situations. The experiments and results are discussed next.

For these experiments, the probe was mounted as shown in Fig. 2 (see side view) with the plane of the probe's measurement triangle in the XZ plane. Note that this orientation of the probe is different from that shown in Fig. 1; the probe is placed in the orientation shown in Fig. 2 only to test the linearity error. For normal measurements, the probe is oriented as shown in Fig. 1.

A ceramic gage block (referred to as 'part' in this section) was positioned on the linear stage and as close as possible to the probe. The part was then moved along the X axis in increments of 0.2 mm over the full travel of 10 mm, and the probe reading was obtained at each position. Because the positioning accuracy of the stage was verified previously with a laser interferometer to be less than $0.5 \mu\text{m}$ over 10 mm, the errors in the probe are simply the difference between the probe's readings and the X axis encoder readings.

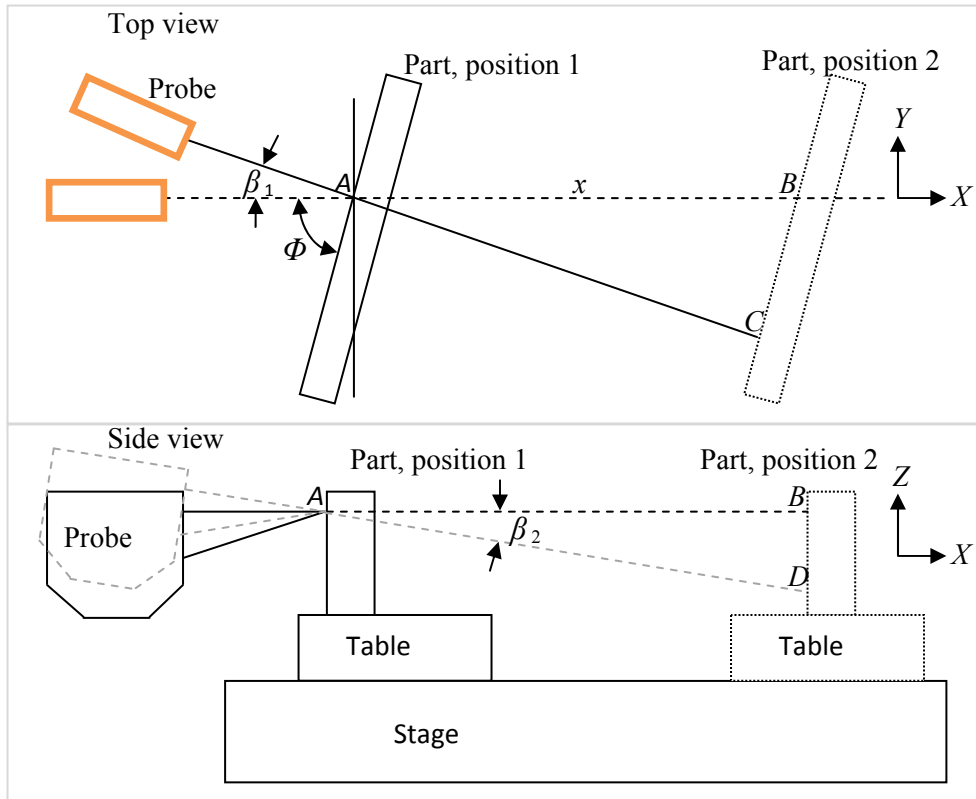


Fig. 2 Schematic of the setup to determine linearity errors for different part orientations

One of the objectives in our testing was to determine linearity errors when the probe's laser is not normally incident on the surface. We therefore intentionally rotated the part by an angle Φ in the XY plane as shown in Fig. 2 (top view). This rotation simulates the measurement of the side wall of a part with the probe tilted as in Fig. 1 (b). A consequence of this intentional rotation is that considerable care must now be taken in aligning the probe in the XY plane because even small misalignments can cause large errors. If the probe is misaligned by angle β_1 with the X axis as shown in the top view in Fig. 2 and the measurement surface of the part makes an angle Φ with the Y axis, then the error e , given by $AC-AB$, can be shown to be

$$e = \frac{x}{\cos \beta_1} \left(\frac{1}{1 + \tan \beta_1 / \tan \phi} \right) - x \quad (1)$$

For the case of normal incidence, $\Phi = 90^\circ$, the error e is simply given by $e = x/\cos\beta_1$ as expected. If the probe is misaligned by a small amount, say $\beta_1 = 0.1^\circ$, the error e over the travel of 10 mm is less than 15 nm. However, if the part were intentionally rotated so that $\Phi = 25^\circ$, and the probe were misaligned in the XY plane by 0.1° , the error is $-37.3 \mu\text{m}$. This error is due to a misalignment in the setup and should not be interpreted as the probe's linearity error. Misalignment of the probe in the XZ plane (β_2 in Fig. 2 sideview) produces a small error given by $e = x/\cos\beta_2$. This error is not influenced by the angle Φ .

For the case of normal incidence, we show the linearity error without removing the slope in the data because the contribution from β_1 and β_2 to the overall error is extremely small (less than $\pm 0.4 \mu\text{m}$) when the part is aligned so that the angle Φ is within $90^\circ \pm 0.5^\circ$. We can attribute any slope in the data to the actual scale error in the probe. Figs. 3 and 4 show the errors for two identical probes from the same manufacturer and for two different materials. Notice that the linearity error is different for both probes and exceeds the manufacturer's specification of $\pm 5 \mu\text{m}$ for the non-ceramic case (graphite).

It should be noted that the pitch motion of the stage can potentially tilt the part to bringing it closer or farther away from the probe, thus producing an error in the measurement that would be convolved with the probe's linearity error. However, the table's pitch specification is 17 arc-seconds over the 600 mm travel. Because pitch errors do not vary rapidly over short travel, and assuming only half this pitch error occurs at 25 mm from the table top, the error due to pitch is approximately $1 \mu\text{m}$. We therefore believe that most of the error seen in Figs. 3 and 4 are due to the probe, and not due to motion errors.

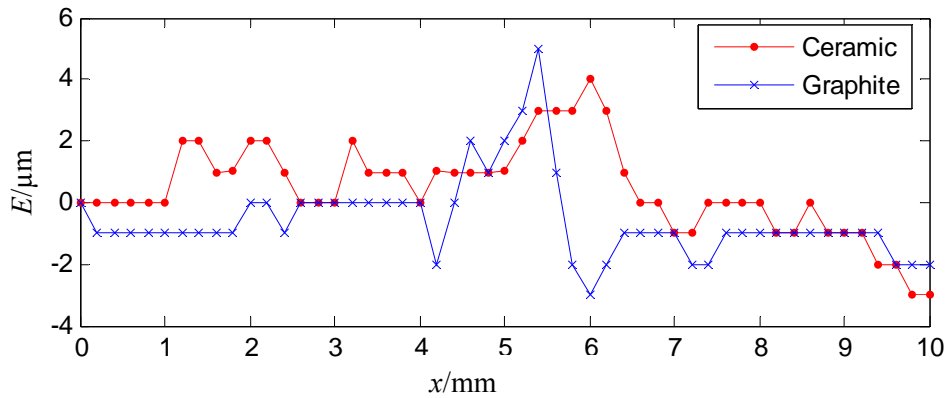


Fig. 3 Linearity errors when $\Phi = 90^\circ$ for probe # 1

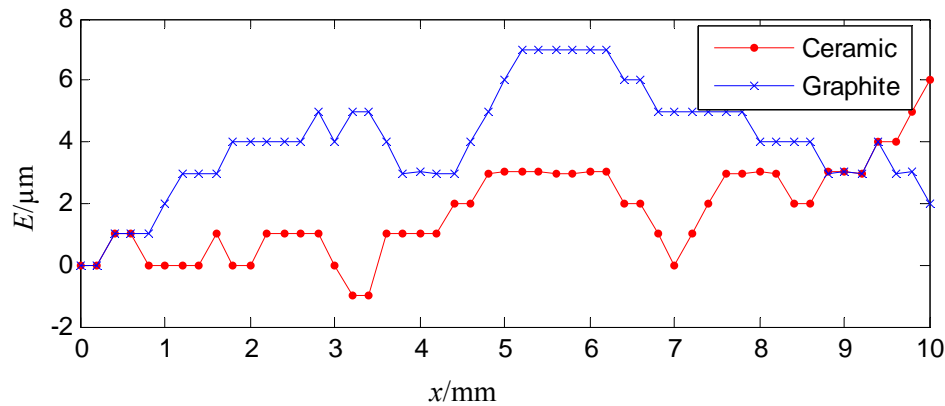


Fig. 4 Linearity errors when $\Phi = 90^\circ$ for probe # 2

For the case where $\Phi = 25^\circ$, we show the measured errors before removing the slope in Fig. 5 and after removing the slope in Fig. 6. As explained earlier, we attribute the slope in Fig. 5 to a misalignment of the probe; a 1° misalignment can produce errors as large as $400 \mu\text{m}$ over 10

mm. Fig. 6 shows that the linearity errors can be larger than the manufacturer’s specification for non-ceramic surfaces.

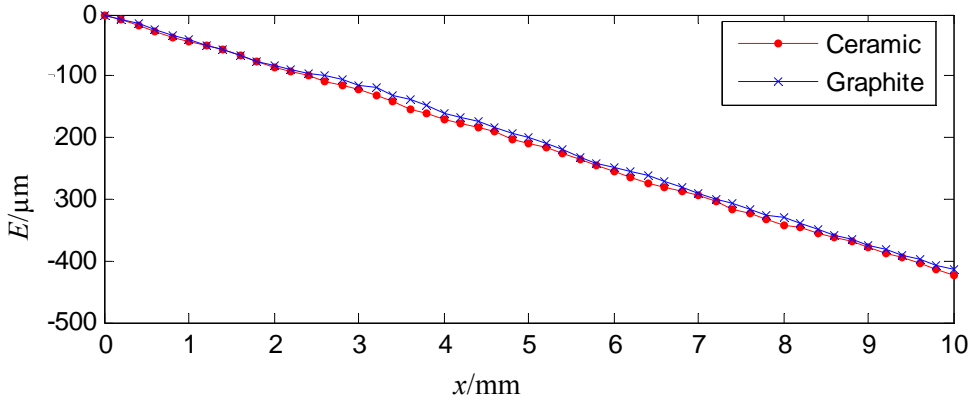


Fig. 5 Linearity errors when $\Phi = 25^\circ$ for probe # 1 before removing the slope

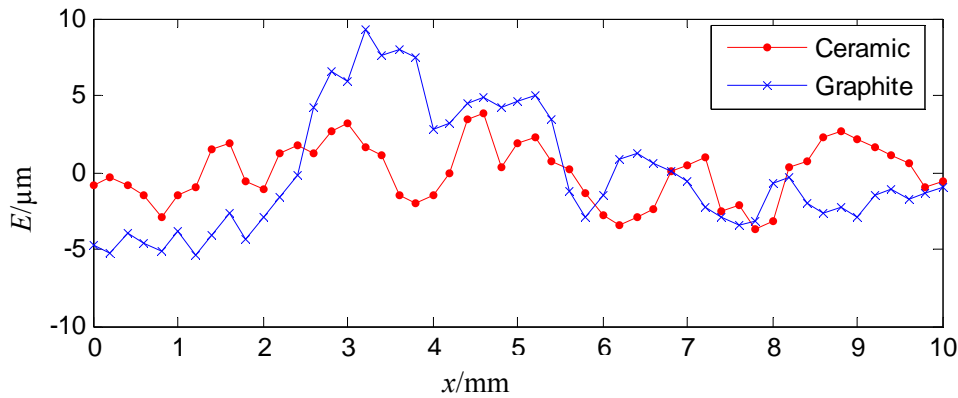


Fig. 6 Linearity errors when $\Phi = 25^\circ$ for probe # 1 after removing the slope

We should note that similar linearity testing has been reported by Fan [7] where they tabulate the errors as a function of both the inclination of the part and for different part colors. However, there are two aspects to their study that differentiate our results from theirs. First, they do not detail the influence of alignment errors in their measurements which can be significant as we have shown. Second, their probe was oriented perpendicular to ours; that is, the plane of the measurement triangle was in the XZ plane (unlike ours in Fig. 1(e) where it is in the YZ plane), while the travel axis continued to remain along the X axis. We explicitly did not consider this case because orienting the probe in the XZ plane will diminish our ability to detect edges; detecting edges is critical to estimating width.

Implications for dimensional measurements: The results show large changes in the linearity error over short travel distances. Fig. 3 shows an error of almost 8 μm over a range that is less than 1 mm for the graphite surface. Therefore, when measuring a step height or channel depth of an artifact (with the probe oriented as in Fig. 1(e)), the positioning of the part within the probe’s range will have substantial effect on the accuracy of the results. For example, if the objective is to measure the height of, say, a 1 mm artifact or a step (gage block or a channel etc), then, we

can do this measurement by placing the artifact at different positions within the range of the probe, since the probe has a 10 mm range. But because the linearity error is larger at about the 5 mm position (mid-range of the probe for probe 1), using the probe at this range to measure a 1 mm height could lead to much larger errors. From Fig. 3, if the part is made of Graphite, and we have one surface of the step at 5.3 mm, and the second surface of the step at 6.3 mm of the probe's range, we could then have at least a 5 μm error in the step. On the other hand, using the probe between its 0.5 mm and 1.5 mm range, we could have practically no error. The manufacturer's specification is only valid for ceramic surfaces under normal incidence. It is likely that the linearity error will exceed the specifications for most practical measurement applications.

3.3 Influence of material/optical properties on height measurements

It is well known that laser triangulation probes are very sensitive to material/optical properties of the components under measurement. The problem of laser surface penetration is pointed out by [6, 8] while volumetric scattering is discussed by [2].

To demonstrate the influence of subtle changes in material/optical properties of the test component on linear dimensional measurements, we considered four ceramic gage blocks that appeared to be visually similar (in terms of color and surface texture). The objective of our experiment is to measure the height of one the blocks under two different conditions as discussed below.

In the first case, we wrung the block on another ceramic block (they were both European blocks but possibly not from the same set) to form a cross-block pair as shown in Fig. 7(a). We obtained a profile across the blocks and calculated the height from that data.

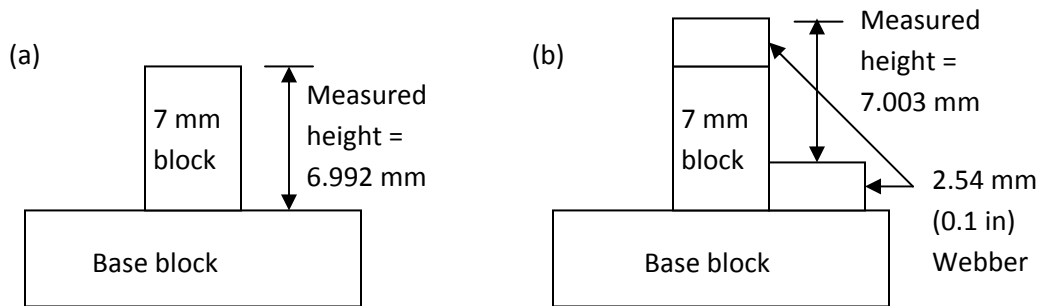


Fig. 7 (a) A crossed block pair to generate a nominal 7 mm height (b) Realizing the same physical length but with different ceramic blocks presented to the probe for measurement

In the second case, we choose two different ceramic blocks of the same height (each is a Webber [10] 0.1-inch) and wrung them to both the bottom and the top block of the cross-block pair. The purpose of doing this is to present a different material to the sensor while maintaining the same physical length. This is shown in Fig. 7(b). We then measured a profile across the blocks and calculated the height. The measured height for case (a) in Fig. 7 was 6.992 mm while the measured height for case (b) was 7.003 mm. There is a difference of 11 μm in the measured height simply by changing the material presented to the probe.

It should be pointed out that if the material/optical properties of the base block and the 7-millimeter ceramic block were identical, then any error will be common-mode between the top and bottom surface and therefore cancel out. The results should then indicate a smaller deviation from the nominal value (which is within a few tens of nanometers of the true value) of 7 mm. That is however not the case here suggesting that the material/optical properties of the base block are different from that of the 7-millimeter block. It is reasonable to assume that the two 0.1-inch blocks are identical in terms of their material/optical properties because the result of that measurement is much closer to the nominal value (the discrepancy of 3 μm is possibly due to error sources in the probe such as its linearity).

Implications for dimensional measurements: Material/optical properties can have a significant influence on the measurement errors as our experiments on visually similar gage blocks reveal. In measuring height, it is extremely critical that the material/optical properties at the two ends of the measurement be identical; otherwise large errors on the order of tens of micrometers are possible.

3.4 Influence of material/optical properties on width measurements

We performed a similar experiment on width measurements using ceramic blocks. For this experiment, we tilted the probe as shown in Fig. 1(b) and obtained a profile from which we determined the position of one side wall of the gage block. A second probe with an opposing tilt was used to acquire data from the opposing side wall. We calculated the width as the difference between the edge positions. However, the probe offset (distance between the probes) is an unknown quantity and therefore this process has to be first performed on a calibrated width. Subsequent to this calibration, we can measure the width of other test blocks. The following paragraphs, data and results are reproduced from [11].

Three ceramic blocks, a 1-inch, 2-inch and 3-inch, were considered for the experiment. Instead of directly measuring the width of the blocks across their side walls, we wrung two thin ceramic blocks to their gaging surfaces and measured the internal distance between the two thin blocks as shown in Fig. 8. The purpose of wringing the thin blocks is to present the same surface for all three gage blocks; therefore, we removed the two thin blocks from the 1-inch block after the measurement and subsequently wrung the same blocks to the 2-inch and 3-inch block for the measurement.

Subsequently, we chose two other sets of two thin blocks and repeated the measurements on the 1-inch, 2-inch and 3-inch blocks. Although all three sets of thin blocks appear to be visually similar, the widths obtained using the different blocks varied considerably. We refer to the thin blocks as European (British Standards blocks), Mitutoyo, and Webber [10].

The results are shown in Table 1. The offset between the probes was calibrated using the 1-inch gage block measured with the thin European blocks. Therefore, that entry (in the first row and first column) has a zero error.

The results indicate that the errors in the measurement of the 1-inch, 2-inch and 3-inch gage blocks are small (less than $\pm 1 \mu\text{m}$) if the probe offset calibration is performed using blocks of similar material. For example, the errors when using the Mitutoyo blocks are $-4.5 \mu\text{m}$, $-4.6 \mu\text{m}$ and $-5.1 \mu\text{m}$ for the 1-inch, 2-inch and 3-inch blocks respectively when using the European 1-inch block as the master. If a Mitutoyo 1-inch block were instead used as the master, the errors for the 2-inch and 3-inch blocks would only be $-0.1 \mu\text{m}$ and $-0.6 \mu\text{m}$ respectively. That is, the range of the errors is small across any row in the table; but the range of errors is large across a column indicating that changing the material seen by the probe can have a large influence on the measured length. For example, the first column shows that if the same 1-inch gage block is measured with three different thin gage blocks of slightly different material properties, we can potentially see large errors, up to $7 \mu\text{m}$, between measurements.

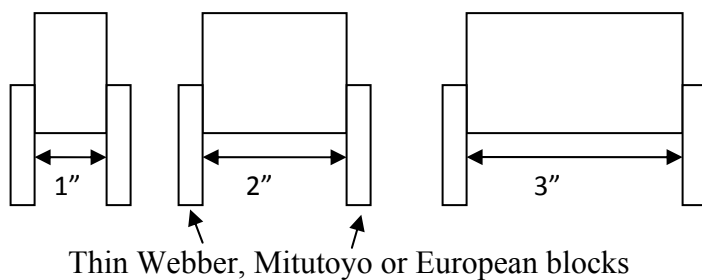


Fig. 8 Width measurements across the gap created using thin blocks

Table 1: Width errors in micrometers

	Nominal	1-inch	2-inch	3-inch
European	0	0.4	1.1	
Mitutoyo		-4.5	-4.6	-5.1
Webber		-7.1	-5.6	-6.1

Implications for dimensional measurements: When using the probe in the configuration shown in Fig. 1(b) for width measurements, it is necessary to calibrate probe offset using a master made of identical material to the part. Otherwise, large errors on the order of $10 \mu\text{m}$ in width measurements are possible.

3.5 Effect of spot size on width measurements

Although the spot sizes of different laser triangulation probes are specified at the center of the range, the size varies significantly at the extremes of the range because the beam is generally conical in shape. In probably its most common setup, the probe is mounted vertically to look straight down on the object under measurement. As the object is scanned, a profile is generated from which height measurements are generally made. Attempting to infer width information from such profiles will be prone to errors because some portion of the beam will still strike the top surface of the block (and therefore be sensed by the probe) even as the center of the beam is just outside the block. This is shown for three different cases in Fig. 9 for a nominal 0.3 in (7.62 mm) gage block. The measured widths for the three cases are shown in Table 2. The measured widths could deviate from the expected width (column 4 in Table 2) for several reasons: chamfer

in the gage block, probe not positioned exactly at the range values indicated in the table, spot size of the probe deviating from the expected values in the table, etc.

Table 2: Effect of finite spot size on measured width of gage blocks, all units in millimeters

Case	Range	Spot size ¹	True width	Approximate expected width	Measured width	Width error (Measured-True)
a	0	0.03	7.62	7.68	7.664	0.044
b	+5	0.25	7.62	7.87	7.848	0.228
c	-5	0.25	7.62	7.87	7.864	0.244

¹Note that the spot sizes are the nominal values as specified by the manufacturer

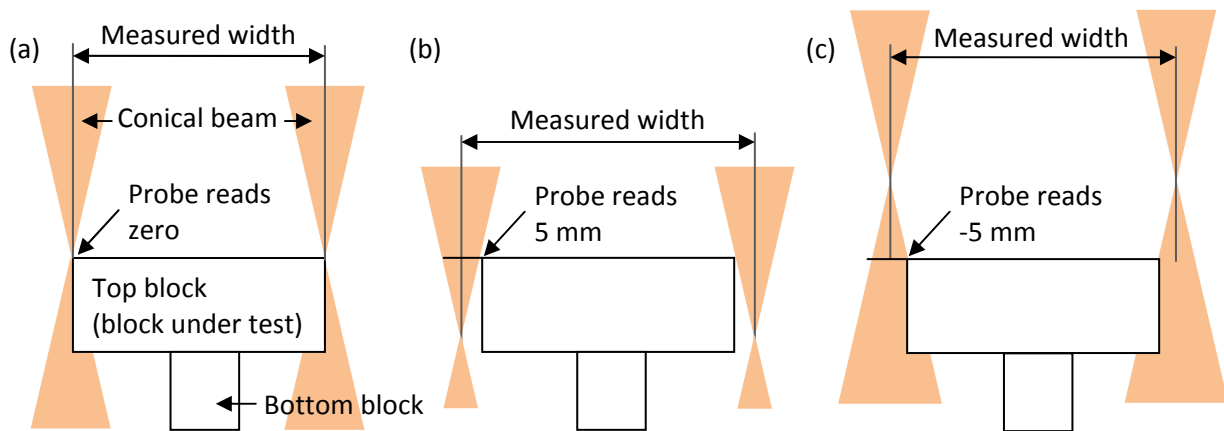


Fig. 9 The effect of different spot sizes on width measurements (a) The probe is focused on the top surface (b) The probe is positioned so that it reads 5 mm at the top surface. The spot size is 250 μm at this position. (c) The probe is positioned so that it reads -5 mm at the top surface. The spot size is 250 μm at this position also.

For these experiments, we note that the part is mounted on another block so that any reflection of the beam from the side walls of the gage block does not strike another surface. Secondary reflections are therefore avoided, at least in our case where we have noticed the absence of a second peak in the intensity graph of the return beam. We should note however that Buzinski et al [1] have indicated that some triangulation probes can in fact sense scattered light even from a vertical side wall.

Implications for dimensional measurements: The edge detection capability is limited by the finite size of the spot. In addition, features in the part such as edge chamfer can further deteriorate the probe's ability to detect edges accurately when the probe is mounted to look straight down on the part. We have shown that errors on the order of 250 μm in the width are possible simply by measuring the same width at different ranges of the probe where the spot sizes are different. The measured width appears larger than the true width due to this error source.

3.6 Side wall reflections

We describe here another set of experiments where we attempt to measure the width of gage blocks under different mounting conditions than described in the preceding section. While in the previous case, there was an apparent expansion of the block, there is an apparent contraction in

the block in this case. Unlike in the previous section where the block under test (the top block) was mounted in such a manner as to avoid any reflection from the bottom block, here we mount the test gage block (the top block) on another gage block (the bottom block) so that the reflected beam from the side wall of the top block strikes the bottom block and the resulting scattered light is sensed by the probe. Two cases where the errors in the measured width are substantially larger than those described in the previous section are shown in Fig. 10.

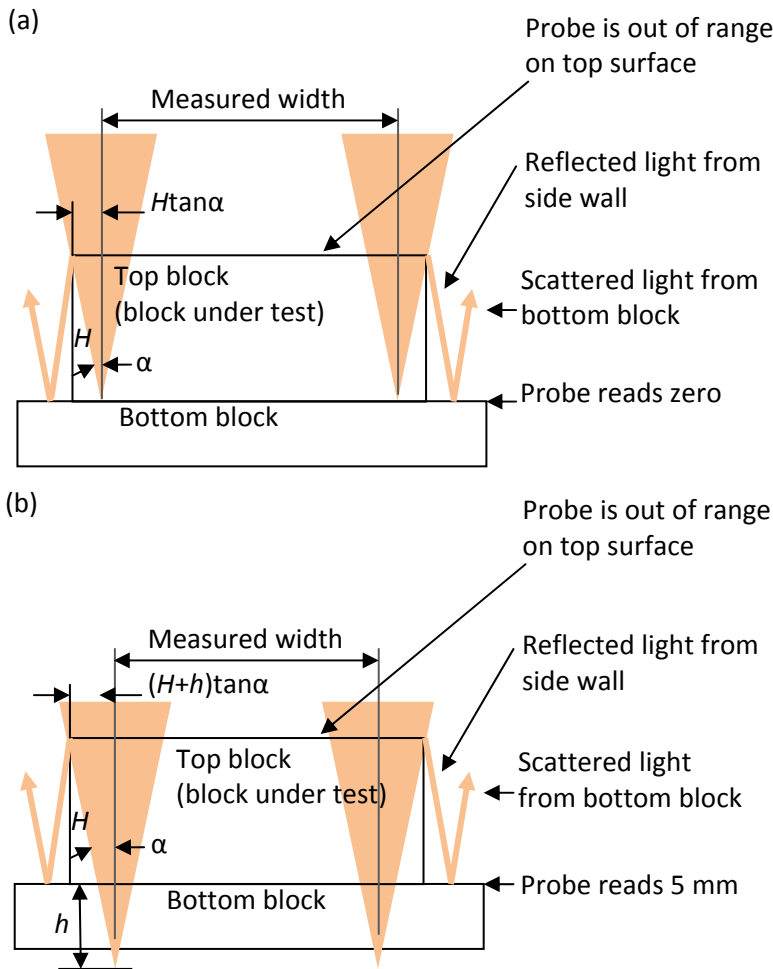


Fig. 10 Side wall reflection resulting in an apparent contraction of the measured width (a) the probe is positioned so that the top surface of the bottom block is at the center of the probe's range. (b) The probe is positioned so that the top surface of the bottom block reads 5 mm (one end of the probe's range).

Case a: The probe is positioned so that the top surface of the bottom block is at the center of the probe's range. The top surface of the block under test is out of the probe's measurement range. From Fig. 10 (a), it can be seen that even if the center of the beam is inside the block under test, some portion of the converging beam strikes the side wall and is reflected to the top surface of the bottom block. The light scattered from this surface is then sensed by the probe. The measured width is therefore much smaller than the true width. We experimentally determined the width to be 7.22 mm, which is 0.4 mm smaller than the nominal. Attributing half the error to each side of

the gage block, the apparent contraction on either side is 0.2 mm. The half angle of the conical beam is 1.26° (calculated from the spot sizes of $30\ \mu\text{m}$ and $250\ \mu\text{m}$ at the center of the probe's range and at 5 mm respectively). The height of the block under test is about 8.8 mm. Therefore, the calculated contraction in width at either end is $8.8\tan(1.26) = 0.194\ \text{mm}$, which is comparable to the experimentally determined value of 0.2 mm.

Case b: The problem described in the previous case is further accentuated when the probe is lowered so that the top surface of the bottom block is at the end of the probe's range (5 mm). We experimentally determined the width to be 7.006 mm for this case, which is 0.614 mm smaller than the nominal. The apparent contraction on either side is 0.307 mm. From the geometry in Fig. 10(b), the calculated contraction is the sum of the value determined in case (a) and half the spot size at 5 mm, which is $0.194 + 0.125 = 0.319\ \text{mm}$. This value is comparable to the experimentally determined value of 0.307 mm.

Implications for dimensional measurements: Determining the edge position in presence of side wall reflections followed by scattering from a secondary surface can lead to even larger errors than that described in section 3.5. If the reflected beam from the side wall has an opportunity to strike another surface, the errors in the width can be as large as $2H\tan\alpha$. For a part that is 25 mm tall, the error can be as large as 1 mm. The measured width appears to be smaller than the true width due to this error source.

3.7 Secondary reflection

Secondary reflection near the intersection of surfaces produces a second peak in the intensity graph of the return beam. While probe manufacturers generally provide some scheme to detect the dominant peak and therefore attempt to eliminate the effect of the secondary reflection, the problem nevertheless persists in many practical applications.

Example 1: Gage block width measurement

In an experiment that combines the issues described in the previous two sections, we attempt to measure the width of a gage block under the situation shown in Fig. 11(a) where the center of the probe is approximately at the half-height of the block. Under this situation, the probe can sense both the top surface of the top block and also the top surface of the bottom block (due to reflection from the side wall). In an ideal case, the apparent expansion due to a finite spot size and the apparent contraction due to side wall reflection serve to cancel each other. In practice, there is still some small error.

In Fig. 11, as the center of the beam is aligned with the vertical edge of the side wall, exactly half the beam (of width equal to $(H-h)\tan\alpha$) strikes the top surface and the resulting scattered light is sensed by the probe. The other half of the beam is reflected off of the side wall and strikes the bottom surface. The scattered light from this surface is also sensed by the probe. There are therefore two peaks in the return intensity graph of the beam. Fig. 11(a) shows the schematic of the setup while Fig. 11(b) shows the dual peak in the intensity graph of the return beam.

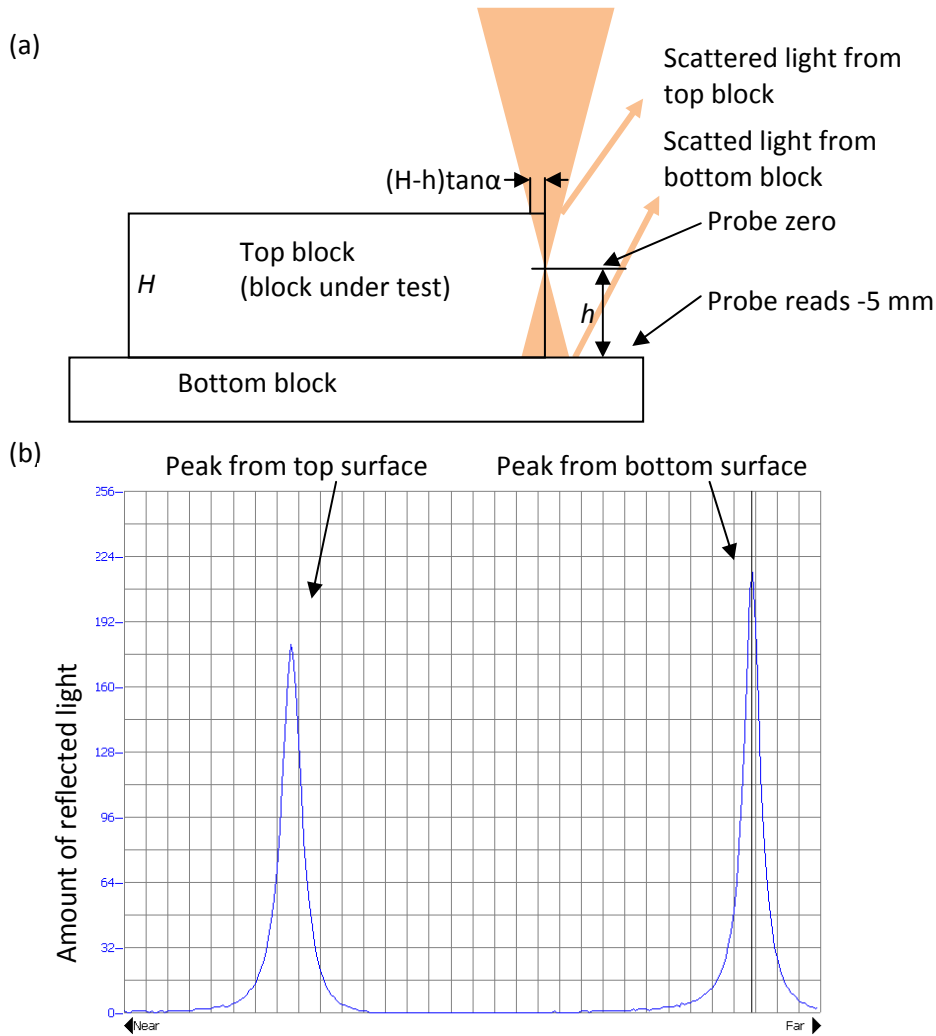


Fig. 11 (a) Width measurement in presence of secondary reflections (b) Dual peak in the intensity graph of the return beam

In an ideal case, the software identifies the dominant peak to determine where the center of the spot actually lies. But this determination may be influenced by many other factors such as edge chamfer, subtle changes in optical properties between the bottom and top surface, the reflectivity of the side wall, etc. In our experiments, we measured a width of 7.583 mm in this case, which is only 37 μm smaller than the nominal width. Given the number of factors that can potentially influence the edge determination, and therefore the width, this appears to be a reasonably small error.

Example 2: Fuel cell channel measurement

In Fig. 12, we show the data acquired near the intersection of two perpendicular surfaces. The curvature in the vertical surface is an artifact of the measurement (we confirmed this by performing measurements on the same artifact using a coordinate measuring machine with a fiber probe). The intensity graph of the return beam did demonstrate two peaks in that region but the software could not clearly discern the true surface location, as the resulting data suggests. This data near the intersection demonstrates a limitation of triangulation probes.

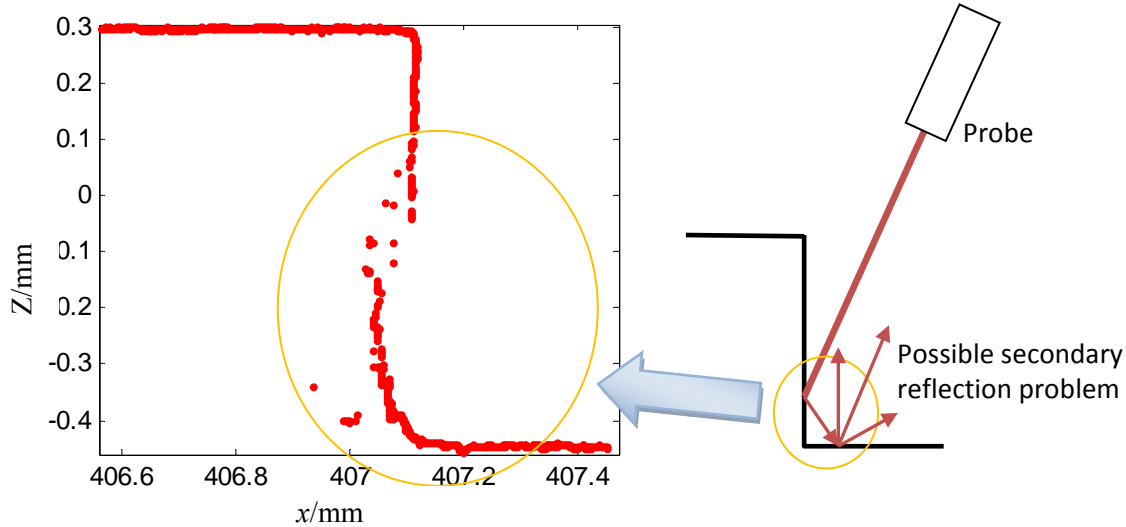


Fig. 12 Data near the intersection of two perpendicular surfaces shows an error in the measurement due to possible secondary reflections.

Implications for dimensional measurements: Avoiding secondary reflections is a major challenge when attempting to perform high accuracy measurements with triangulation probes. In the example of the fuel cell plate, the data on the vertical wall clearly reveals the extent of the problem. If only the top part of the vertical edge is considered in determining the location of the edge, that value is approximately 407.1 mm. If however, some portion of the bottom part is considered instead, that value may be as small as 407.05 mm, or a difference of about 50 μm .

3.8 Measurements at grazing angle

We mentioned in section 3.2 that the linearity specification for the probe is only valid for the case of normal incidence and a white ceramic target. We showed how the linearity error can increase when the part is inclined at steep angles. We presented data for the case of normal incidence where $\Phi = 90^\circ$ (see Fig. 2) and for the case when $\Phi = 25^\circ$. Here, we present the results of measurements made on even steeper angles.

Figure 13 shows the deviations from a least squares best fit line of profiles measured on a white ceramic gage block (the gaging surface is vertical, i.e, it is in the YZ plane) with the probe inclined at different angles (as in Fig. 1(b)). Because the block itself has negligible flatness, the

deviations shown in the data can be attributed to the probing system. It can be seen that as the angle decreases (the beam tends to be grazing the surface), the amplitude of the deviations increases significantly. The range of the data for the case of 10° is more than $40\ \mu\text{m}$. For the 30° case, the range is approximately $10\ \mu\text{m}$ which is just within the specification for the probe. Note that the profiles acquired at the different angles are plotted on the same graph and to avoid overlapping with each other, they are staggered in Y . The error in the measurement is the peak-to-valley of each profile, or the range. The Y position of the profile is of no consequence.

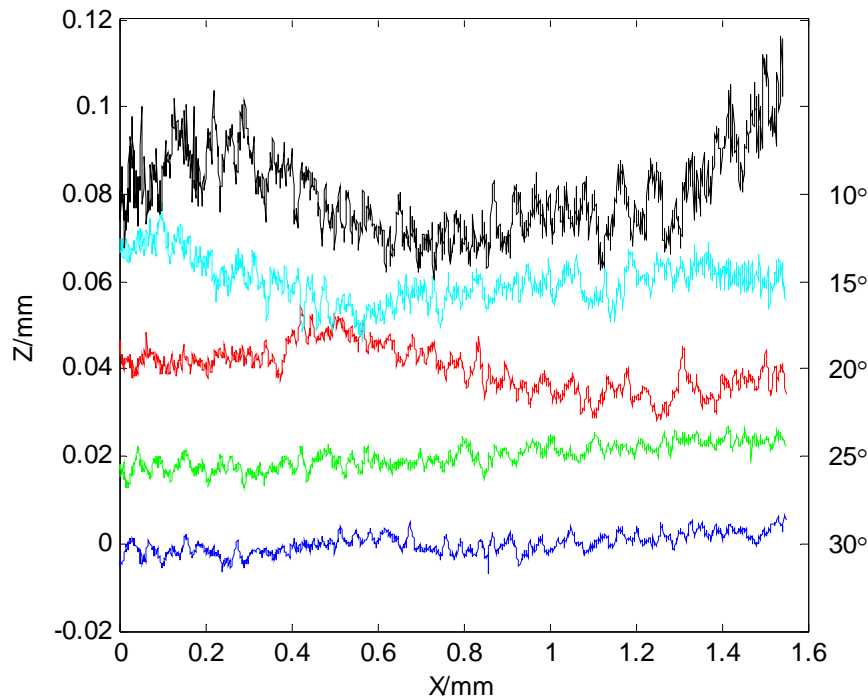


Fig. 13 Profile measurements of a vertical surface (ceramic gage block) with different tilt angles of the probe as in Fig. 1(b). A tilt angle of zero implies that the incident beam is grazing the surface while a tilt angle of 90° implies that the beam is normal to the surface.

Implications for dimensional measurements: If measurements are made at near-grazing angles, the results must be interpreted with caution as a significant portion of the error may be due to the probing system. We have demonstrated errors as large $\pm 20\ \mu\text{m}$ in profile measurements made at 10° angle on white ceramic surfaces.

4 Issues specific to Keyence LK-G32 probe and LK-GD500 controller

In this section, we describe some issues that are specific to the Keyence LK-G32 probe and the LK-GD500 controller.

4.1 Analog output from the controller

As mentioned earlier in this report, we sample the analog output from the probe's controller to synchronize the encoder positions and the probe readings. This output however, is not a true analog signal; rather, it is the digital display value in the controller converted to an analog output.

Fig. 14 shows evidence of this claim. With the probe vertically looking down, we measured an inclined surface at two different Keyence sampling rates. The Keyence sampling rates were set in the Keyence software and determine the frequency at which the controller acquires data. The analog port simply reads the current value of the controller output; it does not sample the probe directly. The part was scanned at a speed of 80 mm/s. At the 50 μs sampling rate, the controller updates a data point every 4 μm . At the 1 ms sampling interval, the controller updates a data point every 80 μm .

In both cases, we attempt to sample a data point every 1 μm via the analog output port of the controller. This sampling interval is smaller than the interval at which the Keyence controller actually acquires a data point in both cases. We would therefore expect to see, and indeed do see (Fig. 14), a stair step pattern in the resulting data where the flat portion in the data is simply multiple samples at the same digital display value. The jump to the next value occurs when the Keyence controller does indeed acquire a new data point.

This stair step pattern is much clearer for the case of the 1 ms sampling as Fig. 14 clearly shows. The analog output only updates to a new value every 80 μm as expected.

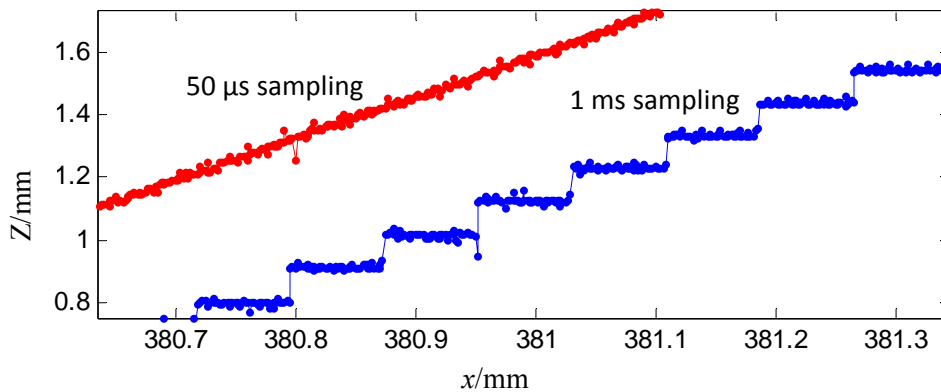


Fig. 14 Measurement of an inclined, but flat, surface at two different Keyence sampling intervals, 50 μs and 1 ms. The part was scanned at 80 mm/s. The stair step pattern, clearly visible for the 1 ms case, shows that although the analog output was sampled every 1 μm , the controller only updates a data point every 80 μm which corresponds to 1 ms at 80 mm/s.

4.2 Delay

Figure 14 also shows another interesting effect, namely, a shift in the data collected at 1 ms in comparison to the data collected at 50 μs . This shift is the result of a delay in acquiring the data by the Keyence controller and the delay increases as the sampling rate increases. We should note that the data was acquired in the negative X direction and therefore, as the delay increases, the probe acquires a data point from a lower elevation, and therefore sees a lower height value.

In general, this delay is not a problem for profile measurements made on a single artifact because such measurements are made at a single sampling rate. In our measurements, we calculate parameters such as width of channels or width of a gage block from such a profile measurement. If different sampling rates are to be used, care must be taken in addressing this delay, as they can lead to potentially large errors in dimensional measurements. It is possible to add fiducials on the surface if measurements have to be performed at different speeds, so as to later tie the data to a common frame.

4.3 Software issues such as alarm, averaging, etc

Another consequence of the analog output being a copy of the digital display is that any software settings such as averaging, sampling rate, alarm levels etc., that impact measurements made via the Keyence software also impact the analog output. For example, the software permits the user to set the number of samples that can be averaged to report a data point. In fact, the probe's repeatability specification of 50 nm is valid only when at least 256 samples are averaged to produce a data point. Setting the number of samples to be averaged to anything other than unity in the software produces a time-averaged output by the controller. Because the display value is now a running average, the analog output is effectively a time-averaged output also. In addition, as mentioned earlier, the sampling interval also produces a delay in acquiring a data point. If averaging is also set to any value other than unity, each of the data points acquired to produce this running average suffers from a delay.

The software allows different sampling rates that can be selected, such as 50 μs , 100 μs , 200 μs , etc. The controller only updates a data point at the selected sampling rate. Sampling the analog port at a faster rate produces no new information, simply multiple copies of the previously acquired sample by the controller. The software allows the user to select alarm levels; these are settings on a sliding scale of 1 to 9 that determine whether an acquired data point is a valid data point or an outlier. Again, these settings affect the controller's display value and therefore the analog output.

4.4 Controller noise

When measuring a stationary target, the controller's display value is usually within $\pm 1 \mu\text{m}$ of the nominal value. While we expected similar performance from the analog output port, we were surprised to see a significantly higher level of noise (n) in the output. Figure 15 shows this noise behavior in the analog port of our controller. The analog port was sampled at a rate of 5 μs while the Keyence sampling rate was set at 50 μs . Figure 16 shows that the noise has an amplitude of about $\pm 12 \mu\text{m}$. It is not random; rather, the observed structure in the data is due to a pulse every 50 μs which is the sampling rate of the Keyence probe. Figure 16 shows a smaller segment of the same data clearly revealing the peaks every 50 μs . One peculiarity about this pulse is that it appears to have an amplitude that changes with time, producing the apparent shape seen in Fig. 15. The source of this noise problem was not elaborated by the manufacturer; a replacement controller did not demonstrate this problem.

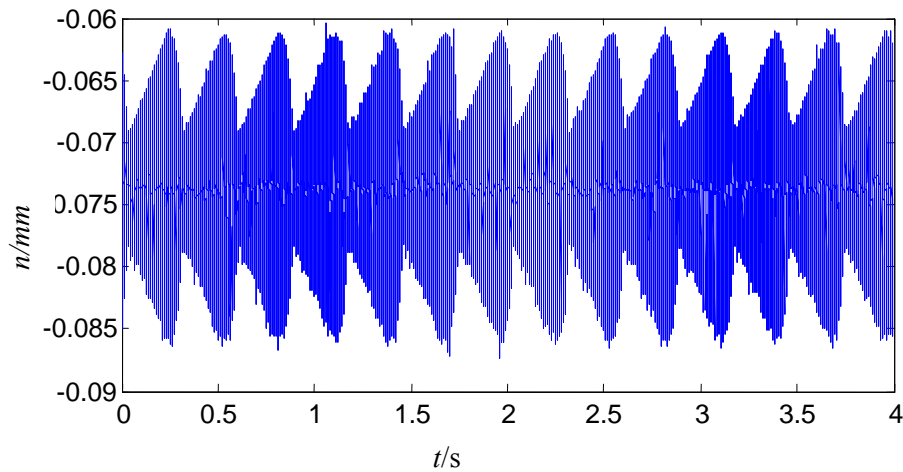


Fig. 15 Noise(n) in the analog output of the Keyence controller. The observed shape in the data is the result of a pulse every $50 \mu\text{s}$. The amplitude of the pulse appears to vary with time in a systematic manner.

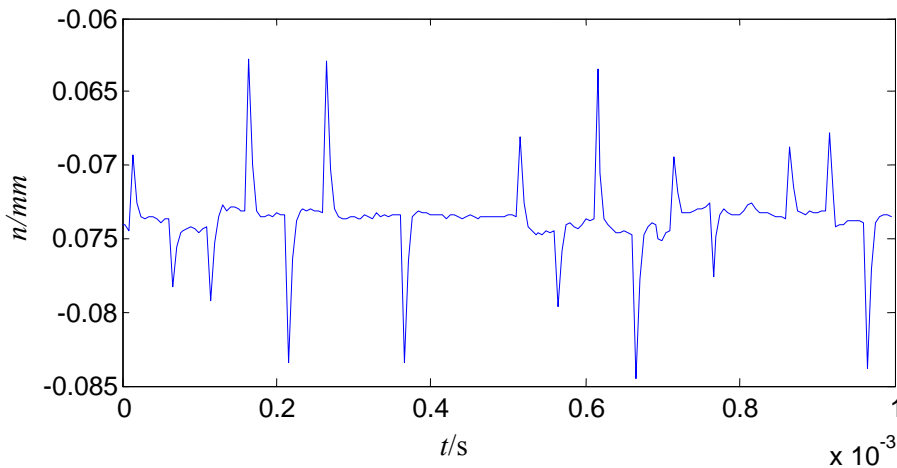


Fig. 16 Noise(n) in the analog output over a short segment showing a pulse every $50 \mu\text{s}$

5 Summary

Measuring linear dimensions such as height and width of an object placed under a laser triangulation probe is probably one of the simplest measurements that can be made with these systems. But even in this simplest of cases, a survey of the literature does not clearly reveal a quantitative assessment of possible errors in such measurements due to “hidden performance attributes” [1] such as the effect of spot size and shape, linearity errors in the probe, etc. We therefore performed several experiments designed to place bounds on errors from numerous influence quantities. We summarize our key observations and results here.

- Probe repeatability specifications (50 nm as specified by Keyence for the LK-G32) are generally valid when a moving average filter is applied. We determined a $\pm 2 \mu\text{m}$ noise level in the data from the analog port of the controller without any filter being applied.

- Linearity errors in the probe are a major error source for height measurements. These errors vary with part inclination and material; we have observed variations of up to 8 μm over just 1 mm of travel.
- Subtle changes in material/optical properties can contribute to errors on the order of tens of micrometers in height and width measurements as we have shown through experiments on ceramic gage blocks.
- The ability to detect edges is limited by the finite size of the spot. The size of the spot itself changes as a function of the range (distance to the part). We have shown errors as large as 250 μm are possible in width estimation when the probe is looking straight down on the part. There is an apparent expansion of the block due to this error source.
- If the reflected beam from the side wall can strike a second surface from which the scattered light is sensed by the probe, larger errors in width are possible. We have shown errors as large as 300 μm are possible, but estimate even larger errors, up to 1 mm, are possible under special cases. There is an apparent contraction of the block due to this error source.
- In some situations where there are secondary reflections, it is possible that the apparent expansion due to finite spot size and apparent contraction due to side-wall reflections cancel each other out. We demonstrated this through an experiment with gage blocks.
- Avoiding secondary reflection is major challenge; we have shown how the side wall data of a fuel cell plate are corrupted by secondary reflections. The error in edge position was shown to be approximately 50 μm in our example.
- When measuring at grazing angles, we have shown noise levels in profile data of gage blocks to be as large as ± 20 μm . Care must therefore be taken in interpreting the results of such grazing angle measurements; a significant portion of this error is due to the probe and not the part.
- Based on our experiments, we recommend that width measurements be performed by tilting the probe as in Fig. 1(b). We have adopted such a scheme in [11] for our fuel cell plate measurements. The limitations imposed by the varying spot size as a function of range is thus avoided. Secondary reflections will still be an issue.
- We also identified a few issues pertaining to our Keyence probe. A major limitation of the probe was that the analog output was actually a copy of the digital display value and therefore any software settings applied to the controller also reflected on the analog port.

Acknowledgements

We gratefully acknowledge the assistance of Patrick Egan at NIST, and associates of Keyence Corporation, National Instruments Inc., and Aerotech Inc. We thank Chris Blackburn and Shawn Moylan at NIST for reviewing this report. We also sincerely thank the two anonymous reviewers of the journal for their very constructive comments.

References

1. Buzinski, M., Levine, A., Stevenson, W.H., Performance characteristics of range sensors utilizing optical triangulation, IEEE 1992 National Aerospace and Electronics Conference, 1230-1236 (1992).

2. A. Garces, D. Huser-Teuchert, T. Pfeifer, P. Scharsich, F. Torres-Leza, E. Trapet, Performance test procedures for optical coordinate measuring probes, Final project report, part 1, July 1993, European Communities Brussels, Contract No. 3319/1/0/159/89/8-BGR-D (30)
3. Xi, F., Liu, Y., Feng, H.-Y., Error compensation for three-dimensional laser scanning data, *Int. J. Adv. Manuf. Technol.*, 18, 211-216 (2001).
4. Nick Van Gestel, Steven Cuypers, Philip Bleys, Jean-Pierre Kruth, A performance evaluation test for laser line scanners on CMMs, *Optics and Lasers in Engineering* 47(2009)336–342
5. Gabriele Guidi, Fabio Remondino, Giorgia Morlando, Andrea Del Mastio, Francesca Ucheddu, Anna Pelagotti, Performance evaluation of a low cost active sensor for cultural heritage documentation, *Optical 3-D measurement techniques VIII*, ISBN 3-906467-67-8, Vol 2, 2007, pp 59-69
6. Gabriele Guidi, Michele Russo, Grazia Magrassi and Monica Bordegoni, Performance Evaluation of Triangulation Based Range Sensors, *Sensors* 2010, 10, 7192-7215
7. K-C Fan, A non-contact automatic measurement for free-form surfaces, *Computer Integrated Manufacturing Systems*, 10 (4), p 277-285, 1997
8. Godin, G., Rioux, M., Beraldin, J.-A., Levoy, M., Cournoyer, L., 2001: An Assessment of Laser Range Measurement of Marble Surfaces. *Proceedings of the 5th Conference on Optical 3-D, Measurement Techniques*, pp. 49-56, Vienna, Austria
9. Christopher Blackburn, Toward a standardized approach for the evaluation of hand-held laser scanner performance, presentation given at the ACMC Annual Workshop, June 2008, Windsor, Ontario Canada.
10. Commercial equipment and materials are identified in order to adequately specify certain procedures. In no case does such identification imply recommendation or endorsement by the National Institute of Standards and Technology, nor does it imply that the materials or equipment identified are necessarily the best available for the purpose.
11. Bala Muralikrishnan, Wei Ren, Dennis Everett, Eric Stanfield, and Ted Doiron, Dimensional Metrology of Bipolar Fuel Cell Plates Using Laser Spot Triangulation Probes, *Measurement Science and Technology*, accepted and in press.